REPORT DOCUMENTATION PAGE

Form Approved
OMB No. 0704-0188

PLEASE DO NOT RETURN YOUR FORM TO THE ABOVE ORGANIZATION.

1. REPORT DATE *(DD-MM-YYYY)*	2. REPORT TYPE	3. DATES COVERED *(From - To)*
07-07-2006	Conference Proceeding (not refereed)	

4. TITLE AND SUBTITLE

Properties of Shallow Water Environments Retrieved from Hyper-and-Multi-Spectral Space-Borne Sesnors

5a. CONTRACT NUMBER

5b. GRANT NUMBER

5c. PROGRAM ELEMENT NUMBER

6. AUTHOR(S)

ZhongPing Lee, Brandon Casey, Robert Arnone, Rost Parsons, Alan Weidemann and Wesley Goode

5d. PROJECT NUMBER

5e. TASK NUMBER

5f. WORK UNIT NUMBER

73-8669-05-5

7. PERFORMING ORGANIZATION NAME(S) AND ADDRESS(ES)

Naval Research Laboratory
Oceanography Division
Stennis Space Center, MS 39529-5004

8. PERFORMING ORGANIZATION REPORT NUMBER

NRL/PP/7330-05-5189

9. SPONSORING/MONITORING AGENCY NAME(S) AND ADDRESS(ES)

NASA Headquarters
Suite 1M32
Washington, DC 20546-0001

10. SPONSOR/MONITOR'S ACRONYM(S)

NASA

11. SPONSOR/MONITOR'S REPORT NUMBER(S)

12. DISTRIBUTION/AVAILABILITY STATEMENT

Approved for public release, distribution is unlimited.

13. SUPPLEMENTARY NOTES

14. ABSTRACT

There are two imagers on NASA EO-1 satellite: Hyperion and Advanced Land Imager (ALI). Hyperion is a hyperspectral sensor with about 45 bands covering the spectral range of 430 - 900 nm, while ALI has only six (wide width) bands for the same range. Past studies have shown that data from both kinds of sensors can provide observations of important environmental properties, such as bathymetry and water turbidity. In the derivation of bathymetry using data from multi-band sensors (e.g., LANDSAT), however, usually bathymetry data of few locations were required to be known first. Recently, a semi-analytical spectral optimization algorithm has been derived without a priori knowledge of depths at a few locations, and properties of water column and bottom can be retrieved simultaneously from remotely sensed data. In this study, we extend tha optimization approach to ALI data, with retrieved water and bottom properties compared with that from Hyperion data. From these results, we discuss the advantages of Hyperion and ALI sensors, and their potential applications for coastal observations.

15. SUBJECT TERMS

EO-1, remote sensing, shallow coastal water

16. SECURITY CLASSIFICATION OF:			17. LIMITATION OF ABSTRACT	18. NUMBER OF PAGES	19a. NAME OF RESPONSIBLE PERSON
a. REPORT	b. ABSTRACT	c. THIS PAGE			ZhongPing Lee
Unclassified	Unclassified	Unclassified	UL	7	19b. TELEPHONE NUMBER *(Include area code)* (228) 688-4873

8th International Conference on Remote Sensing for Marine and Coastal Environments

17–19 MAY 2005 • HALIFAX, NOVA SCOTIA CANADA

Properties of shallow water environments retrieved from hyper- and multi-spectral space-borne sensors*

ZhongPing Lee, Brandon Casey, Robert Arnone, Rost Parsons, Alan Weidemann, Wesley Goode
Naval Research Laboratory, Code 7333
Stennis Space Center, MS 39529

ABSTRACT

There are two imagers on NASA' EO-1 satellite: Hyperion and Advanced Land Imager (ALI). Hyperion is a hyperspectral sensor with about 45 bands covering the spectral range of 430 – 900 nm, while ALI has only six (wide width) bands for the same range. Past studies have shown that data from both kinds of sensors can provide observations of important environmental properties, such as bathymetry and water turbidity. In the derivation of bathymetry using data from multi-band sensors (e.g., LANDSAT), however, usually bathymetry data of a few locations were required to be known first. Recently, a semi-analytical spectral optimization algorithm has been developed for remote-sensing of shallow-water environments. Using data from hyperspectral airborne and space-borne sensors, it has been demonstrated that bathymetry of optically shallow waters can be derived without *a priori* knowledge of depths at a few locations, and properties of water column and bottom can be retrieved simultaneously from remotely sensed data. In this study, we extend the optimization approach to ALI data, with retrieved water and bottom properties compared with that from Hyperion data. From these results, we discuss the advantages/disadvantages of Hyperion and ALI sensors, and their potential applications for coastal observations.

Keywords: EO-1, remote sensing, shallow coastal water

1. Introduction

There are two imagers on NASA' EO-1 satellite: Hyperion and Advanced Land Imager (ALI). Hyperion is a hyperspectral sensor with about 45 bands covering the spectral range of 430 – 900 nm, but ALI has only six (wide width) bands for the same spectral domain (see Fig.1). However, the swath of Hyperion is about 7 km, but ALI has a swath of ~30 km that provides much more spatial observations than Hyperion. Such a spectral and spatial configuration motivated us to find effective ways of using ALI data to retrieve properties of coastal-water environments.

Past studies have shown that data from hyperspectral sensor alone is adequate for the derivation of water column and bottom properties [1, 2]. When using data from multiple spectral band (e.g., LANDSAT), however, usually *a priori* knowledge of the bottom or the water column are required to derive a bathymetry map from data of multi-band imager [3, 4]. Such a requirement may not be met for some military operations. Therefore it is desired to find a technique that has similar capabilities as the hyperspectral sensor.

In this study, with concurrent measurements of Hyperion and ALI over Looe Key (Florida), we revised the spectral optimization approach designed for hyperspectral sensors and applied it to the ALI data, and compared the derived bathymetry and water properties from both sensors. The results indicate that such an optimization technique is reasonable for area with shallow bathymetry (< 3 m), but could result large errors for deeper bottom (> 10 m). More studies are required to improve the reliability of using ALI data to derive bathymetry of deeper area.

---

* The 8th International Conference for Marine and Coastal Environments, Halifax, Nova Scotia, May 17-19, 2005.

2. DATA AND METHODS

L1A Hyperion and ALI data over Looe Key (Florida) collected on October 26, 2002 was provided by the USGS. Figure 2 presents a subset of the imaged area. Hyperion coverage is generally overlapping with the left portion of ALI coverage. Since the swath of Hyperion is much narrower than that of ALI, only the overlapping portions of Hyperion and ALI were considered in this study (see Fig. 3). The two vertical lines in Fig.3 (colored white and green in both images) were selected to compare the retrievals from both sensors.

To analytically derive water and/or bottom properties from any remotely-collected data, the first step is to get high-quality data of remote-sensing reflectance (R_{rs}), which is defined as the ratio of water-leaving radiance (L_w) to downwelling irradiance just above the surface (Ed). It is R_{rs} that solely contains water and/or bottom information.

To get R_{rs} from sensor-measured quantity (L_t), an important step is to remove the contributions from the atmosphere. Recently, Lee et al. [5] simplified the cloud-shadow method developed by Reinersman et al. [6] to effectively derive R_{rs} from remotely sensed data. Basically, this method uses adjacent pixels that are in and out of cloud shadow to derive the atmosphere contribution. Further, the approach uses L_t from cloud top as a reference for downwelling irradiance. Using Hyperion data over Looe Key, the method is validated with measurements from ship-borne sensor [5]. We here applied the same approach to data from ALI, and ALI R_{rs} of the interested area is calculated.

Figure 4 compares ALI R_{rs} (red square) with Hyperion R_{rs} (blue line) for a few selected points (marked as p1 – p4 in Fig.3). Also shown are the ALI equivalent R_{rs} (green triangle) converted from Hyperion R_{rs} based on the band width of ALI bands. Generally, for the six ALI bands that have the same central wavelengths as Hyperion, the ALI R_{rs} agree with the ALI equivalent (Hyperion-converted) R_{rs} quite well, though larger differences are found at Band 3. Such results indicate that the method of calculating R_{rs} is effective and valid for ALI data. At this point, it is not clear yet how the traditional atmosphere correction approach [7, 8] would behave for such wide-width and poorly calibrated sensor.

3. RETRIEVAL OF ENVIRONMENTAL PROPERTIES

To derive properties of the water column and bottom from R_{rs}, we took the spectral optimization approach developed by Lee et al. [1, 2]. Briefly, the approach models R_{rs} spectrum as a function of five independent variables for optically shallow waters, i.e.,

$$\begin{aligned} R_{rs}(\lambda_1) &= F(a_w(\lambda_1), b_{bw}(\lambda_1), \boldsymbol{P, G, X, B, H}) \\ R_{rs}(\lambda_2) &= F(a_w(\lambda_2), b_{bw}(\lambda_2), \boldsymbol{P, G, X, B, H}) \\ &\vdots \\ R_{rs}(\lambda_n) &= F(a_w(\lambda_n), b_{bw}(\lambda_n), \boldsymbol{P, G, X, B, H}) \end{aligned}, \quad (1)$$

Here $\boldsymbol{P}$ and $\boldsymbol{G}$ are absorption coefficients of phytoplankton and gelbstoff at 440 nm respectively; $\boldsymbol{X}$ is the backscattering coefficient of suspended particles at 440 nm, $\boldsymbol{B}$ the bottom reflectance at 550 nm, and $\boldsymbol{H}$ the bottom depth. a_w and b_{bw} are the absorption and backscattering coefficients of pure water, respectively, which are known from measurements [9, 10]. To derive the five unknowns, a spectral optimization scheme with computer processing code (HOPE) has been developed. By varying the values of the five unknowns, the five unknown components are considered derived when the modeled R_{rs} spectrum best matches the Hyperion spectrum.

This approach, which solves five independent variables simultaneously, requires a sensor has at least 15 spectral bands covering the 400 – 800 nm range for reliable retrieval of water and bottom properties [11]. ALI R_{rs}, however, has only five wide-width bands covering this domain. To reduce the number of unknowns, we adopted the approach developed by Lee et al. [12] to model the total absorption coefficient of the water column. In this approach, hyperspectral $a(\lambda)$ is modeled as a function of $a(490)$, i.e. by one variable, and then Eq.1 becomes

$$
\begin{aligned}
R_{rs}(\lambda_1) &= F(a_w(\lambda_1), b_{bw}(\lambda_1), \boldsymbol{A}, \boldsymbol{X}, \boldsymbol{B}, \boldsymbol{H}) \\
R_{rs}(\lambda_2) &= F(a_w(\lambda_2), b_{bw}(\lambda_2), \boldsymbol{A}, \boldsymbol{X}, \boldsymbol{B}, \boldsymbol{H}) \\
&\vdots \\
R_{rs}(\lambda_n) &= F(a_w(\lambda_n), b_{bw}(\lambda_n), \boldsymbol{A}, \boldsymbol{X}, \boldsymbol{B}, \boldsymbol{H})
\end{aligned}, \qquad (2)
$$

with $\boldsymbol{A}$ for $a(490)$. Eq.2 is now used to generate a hyperspectral $R_{rs}(\lambda)$, and this $R_{rs}(\lambda)$ spectrum is converted to equivalent ALI $R_{rs}(\lambda_i)$ in accordance with the spectral response function of the ALI sensor. And finally, this $R_{rs}(\lambda_i)$ is compared with the $R_{rs}(\lambda_i)$ derived from ALI data. When the two $R_{rs}(\lambda_i)$ matches each other, the set of values of $\boldsymbol{A}$, $\boldsymbol{X}$, $\boldsymbol{B}$, and $\boldsymbol{H}$ is considered derived. Note that in this process, no *a prior* information is required or used.

4. Results and discussion

To see how retrievals from ALI data compared with retrievals from Hyperion, Figure 5 shows the bathymetry outputs from both sensors that cover the same area. The boxes in Fig.5 show the overlapping coverage from both sensors. Note that the bathymetry from Hyperion R_{rs} for this area has been validated with data from ship measurements and airborne LIDAR [5]. For the bathymetry from ALI R_{rs}, apparently the bathymetry better matches the Hyperion bathymetry for portions where the bottom is quite shallow (upper half of the picture). For the lower half that shows the gradual transition of shallower to deeper bathymetry, the ALI depths do not show a gradual transition and are generally deeper. This phenomenon can also be seen for the two lines marked in Fig.3. For the white line, the two bathymetries matched each other quite well for depths less than ~3.0 meter (about after the position p2). After that, the ALI bathymetry quickly jumps to larger values, though which shows similar patterns as that of Hyperion depth (see Fig.6). Similar result is found for the green line.

For the absorption coefficient at 440 nm ($a(440)$), it is found that $a(440)$ from ALI is systematically smaller than that from Hyperion (see Fig.7). This could be the main reason for deeper depths that were derived from ALI R_{rs}. For passive remote sensing of bathymetry, the absorption (or attenuation) coefficients of the wavelengths that have bottom signals in the measured R_{rs} play important role. For shallower bathymetry (e.g., less than 3 meter), ALI R_{rs} at Band 4 may still have adequate signals from bottom reflectance, and contributes to the derivation of bottom bathymetry. At this band, its absorption coefficient is dominated by the contributions from pure water, therefore less uncertainty in this value. For deeper bathymetry (e.g., greater than 10 meter), the derivation of bottom depth from ALI R_{rs} relies mostly on data at Band 1 and Band 2. The absorption coefficients at these two bands, however, also vary with constituents in the water, in turn resulted bigger errors in bottom bathymetry. Conceptually, if the absorption coefficients are known *a prior* or from other means, bottom depth could be derived more accurately from such multiple-band sensors when the bathymetry is deeper than ~5 meters.

ACKNOWLEDGEMENT

Financial support for this study was provided by NASA. Mr. Todd Taylor of the USGS helped the EO-1 collection and distribution.

REFERENCE

1. Z. P. Lee, K. L. Carder, C. D. Mobley, R. G. Steward, and J. S. Patch, "Hyperspectral remote sensing for shallow waters: 2. Deriving bottom depths and water properties by optimization," Applied Optics **38**, 3831-3843 (1999).
2. Z. P. Lee, K. L. Carder, R. F. Chen, and T. G. Peacock, "Properties of the water column and bottom derived from AVIRIS data," J. Geophy. Res **106**, 11639-11652 (2001).
3. D. R. Lyzenga, "Passive remote-sensing techniques for mapping water depth and bottom features," Applied Optics **17**, 379-383 (1978).
4. R. P. Stumpf, K. Holderied, and M. Sinclair, "Determination of water depth with high-resolution satellite imagery over variable bottom types," Limnol. Oceanogr. **48**(1), 547-556 (2003).

5. Z. P. Lee, B. Casey, R. Parsons, A. Weidemann, and R. Arnone, "Bathymetry and water properties derived from hyperspectral satellite imagery," presented at the Algorithms and Technologies for Multispectral, Hyperspectral, and Ultraspectral Imagery XI, SPIE, Orlando, FL, March 28 - 31, 2005.
6. P. Reinersman, K. L. Carder, and F. R. Chen, "Satellite-sensor calibration verification with the cloud-shadow method," Applied Optics **37**(24), 5541-5549 (1998).
7. H. R. Gordon and M. Wang, "Retrieval of water-leaving radiance and aerosol optical thickness over oceans with SeaWiFS: A preliminary algorithm," Applied Optics **33**, 443-452 (1994).
8. B. C. Gao, M. J. Montes, Z. Ahmad, and C. O. Davis, "Atmospheric correction algorithm for hyperspectral remote sensing of ocean color from space," Applied Optics **39**(6), 887-896 (2000).
9. R. Pope and E. Fry, "Absorption spectrum (380 - 700 nm) of pure waters: II. Integrating cavity measurements," Applied Optics **36**, 8710-8723 (1997).
10. A. Morel, ed., *Optical properties of pure water and pure sea water*, Optical Aspects of Oceanography (Academic, New York, 1974), pp. 1-24.
11. Z. P. Lee and K. L. Carder, "Effect of spectral band numbers on the retrieval of water column and bottom properties from ocean color data," Applied Optics **41**, 2191-2201 (2002).
12. Z. P. Lee, W. J. Rhea, R. Arnone, and W. Goode, "Absorption coefficients of marine waters: Expanding multi-band information to hyperspectral data," IEEE Transactions on Geoscience and Remote Sensing **43**(1), 118-124 (2005).

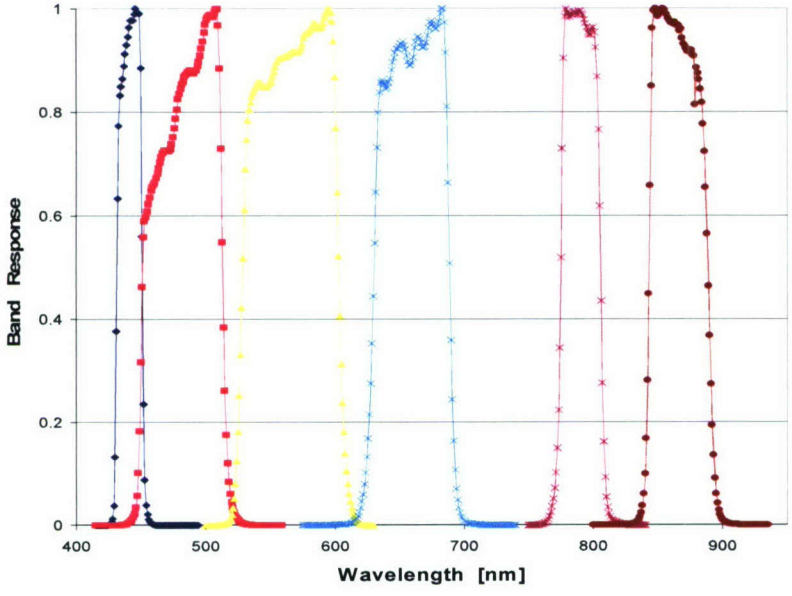

Figure 1. Band and spectral response of the ALI sensor (from http://eo1.usgs.gov/).

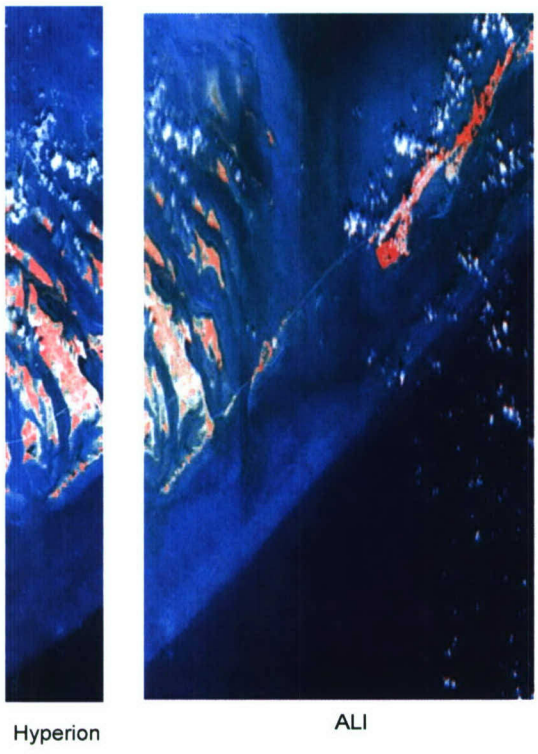

Figure 2. Coverage of Hyperion and ALI for Looe Key (FL).

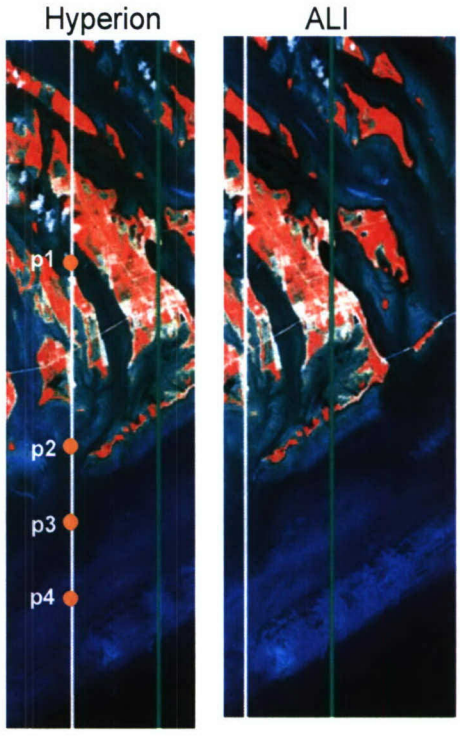

Figure 3. The area focused in this study.

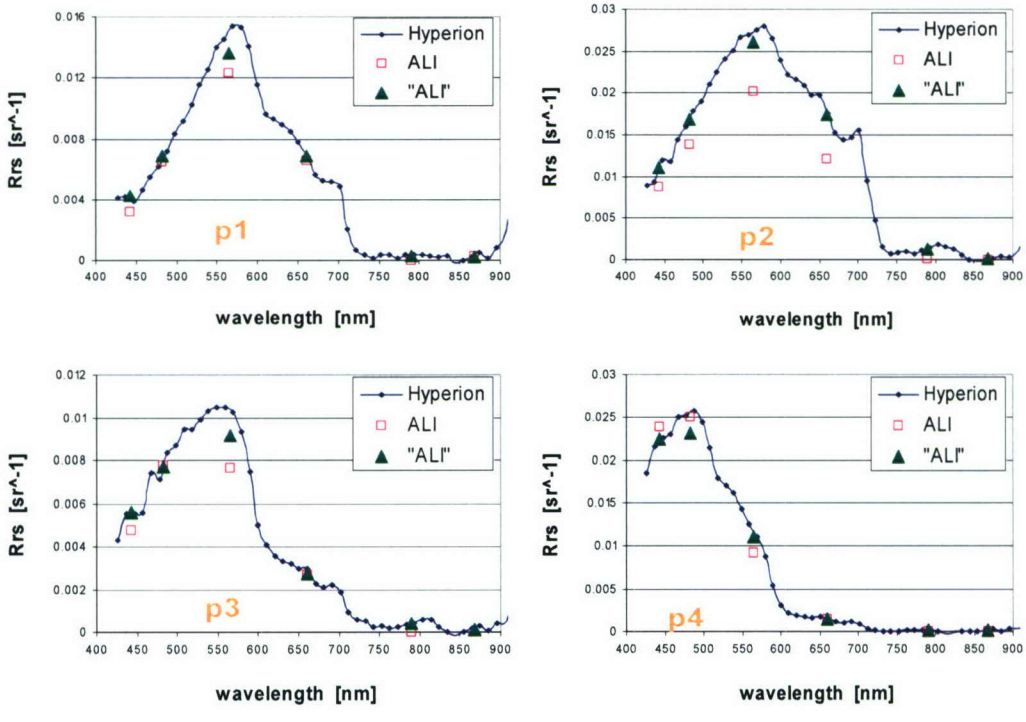

Figure 4. Comparison of ALI R_{rs} (red square) versus Hyperion R_{rs} (blue line). Green triangle indicates the ALI equivalent R_{rs} that is converted from Hyperion R_{rs} based on the ALI band width.

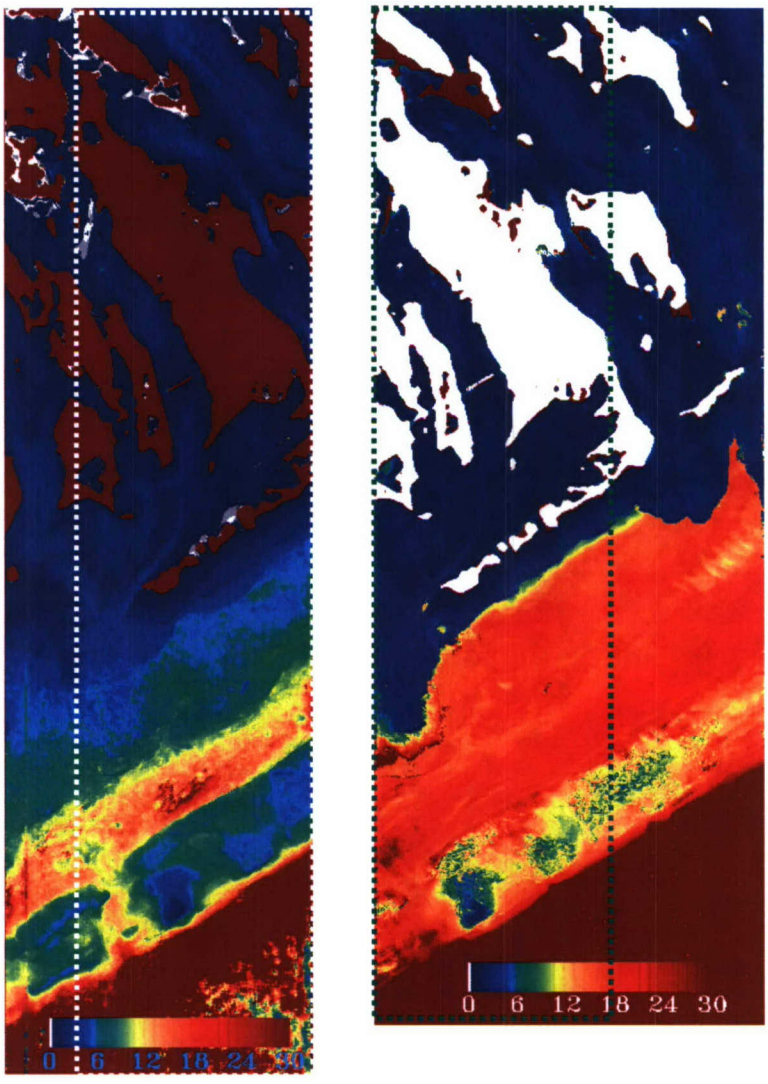

Figure 5. Bathymetry image derived from ALI R_{rs} (right) compared with that from Hyperion R_{rs} (left). Boxes indicate same coverage from both sensors.

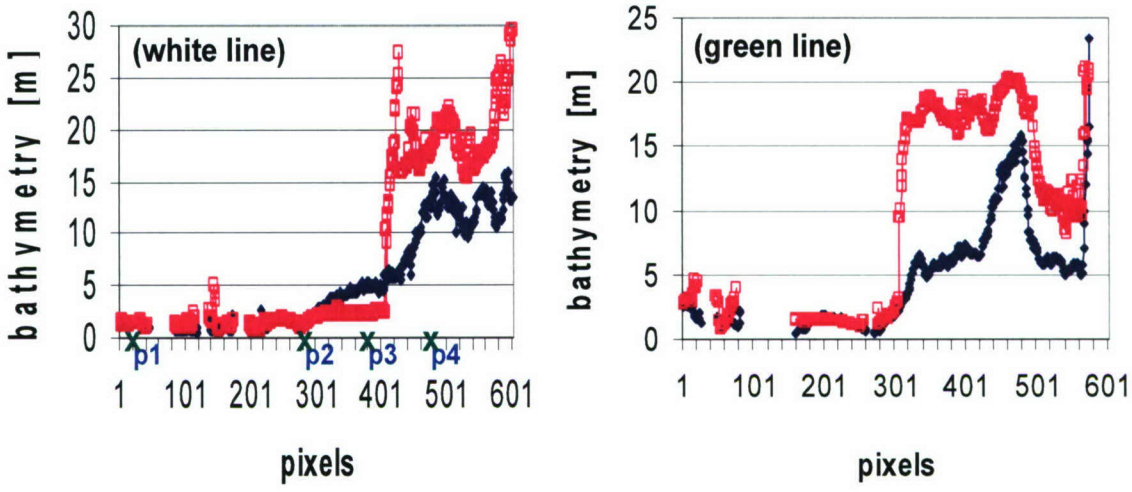

Figure 6. For the lines in Fig. 3, bathymetry from ALI R_{rs} compared with that from Hyperion R_{rs}.

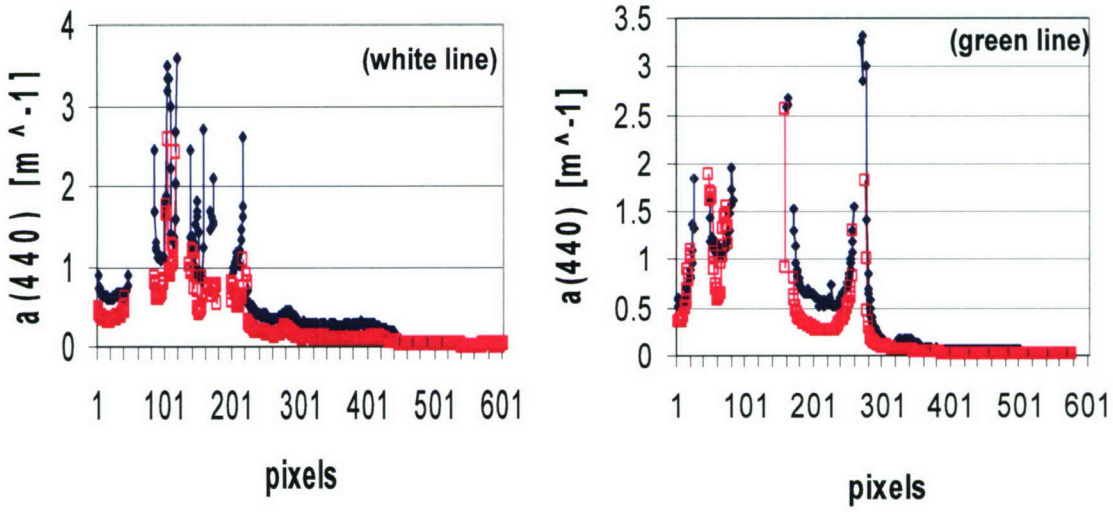

Figure 7. For the lines in Fig. 3, a(440) from ALI R_{rs} compared with that from Hyperion R_{rs}.